

Exact solutions for topological surface states of three-dimensional lattice models

Matias Mustonen,¹ Teemu Ojanen,^{1,2} and Ali G. Moghaddam^{1,2,3}

¹*Computational Physics Laboratory, Physics Unit,*

Faculty of Engineering and Natural Sciences, Tampere University, FI-33014 Tampere, Finland

²*Helsinki Institute of Physics, University of Helsinki, Helsinki FI-00014, Finland*

³*Department of Physics, Institute for Advanced Studies in Basic Sciences (IASBS), Zanjan 45137-66731, Iran*

In this work, we establish a generalized transfer matrix method that provides exact analytical and numerical solutions for lattice versions of topological models with surface termination in one direction. We construct a generalized eigenvalue equation, equivalent to the conventional transfer matrix, which neither suffers from nor requires singular (non-invertible) inter-layer hopping matrices, in contrast to previous works. We then apply this formalism to derive, with exactness, the topological surface states and Fermi arc states in two prototypical topological models: the 3D Bernevig-Hughes-Zhang model and a lattice model exhibiting Weyl semimetal behavior. Our results show that the surface states and bulk bands, across the projected 2D Brillouin zone, agree perfectly with those obtained through direct numerical diagonalization of the corresponding Hamiltonians in a slab geometry. This highlights that the generalized transfer matrix method is not only a powerful tool but also a highly efficient alternative to fully numerical methods for investigating surface physics and interfaces in topological systems, particularly when it is required to go beyond low-energy effective descriptions.

I. INTRODUCTION

One of the distinguishing features of topological phases is the presence of robust boundary states, which are gapless and localized at the boundary of the system [1–7]. Unlike the boundary modes in non-topological insulating states, these surface states persist in the presence of perturbations and disorder, as long as the bulk gap and the corresponding topological insulating phase endure. The existence and robustness of these boundary states are intrinsically tied to the nontrivial topology of the bulk system, demonstrating the phenomenon known as *bulk-boundary correspondence* [8–10]. During the past decade, most theoretical studies have concentrated on obtaining dispersion relations for topological surface states using low-energy effective models [11–15]. Alternatively, most of the works often relied on full numerical methods for tight-binding models and any other realistic lattice models of topological states [16, 17].

The transfer matrix technique has recently been reintroduced for determining topological boundary modes in tight-binding models [18–22]. These methods build on the original concept of calculating a surface’s electronic structure, along with bulk states, by solving recursive equations formulated using the transfer matrix [23–25]. However, most studies to date have focused on applying these methods to two-dimensional (2D) or two-band models, such as the Qi-Wu-Zhang (QWZ) model, which serves as a toy model for the Chern insulating phase [26]. Moreover, recent research has primarily aimed to develop a formalism capable of handling cases with singular (non-invertible) inter-layer hopping matrices. Here, following the original ideas from Ref. [23], we establish a generalized version of the transfer matrix method that inherently avoids the issue of non-invertibility, eliminating the need to treat singular and non-singular cases separately. This approach ensures that our method works effectively for

both singular and non-singular forms of the inter-layer hopping matrix, neither suffering from nor relying on the presence of a singular matrix.

Here, instead of the standard equation in terms of the transfer matrix \mathbb{T} , we construct an equivalent relation with two matrices, \mathbb{S} and \mathbb{R} , such that $\mathbb{R}\mathbb{T} = \mathbb{S}$, with \mathbb{R} being responsible for resolving the non-invertibility issue. Then, we find the eigenvalues and eigenvectors of the generalized eigenvalue problem associated with the two matrices \mathbb{S} and \mathbb{R} . The surface states, as well as the delocalized bulk states, can all be decomposed in terms of the resulting eigenstates. Therefore, by applying the boundary conditions corresponding to surface termination, we derive the necessary and sufficient conditions from which the energies of surface states, as well as the edges of bulk bands (in the projected 2D Brillouin zone of the surface), can be determined. We apply this formalism to well-known lattice models for topological insulators and semimetals, including the 3D Bernevig-Hughes-Zhang (BHZ) model and a minimal two-band model for 3D Weyl semimetals.

It is worth noting that the transfer matrix method is not only a highly efficient alternative to direct diagonalization of real-space Hamiltonians, but in the case of semi-infinite geometries or regions far from surfaces, it serves as the only exact method. Brute-force diagonalization is inherently limited to finite-size systems and can only provide approximate descriptions of semi-infinite or isolated surface states. In contrast, the transfer matrix method offers an exact formalism for studying surface physics in infinite systems, beyond the capabilities of any brute-force approach. Even when analytical evaluation of this exact method is not feasible, the formalism can still be applied numerically, maintaining its efficiency and precision.

II. TRANSFER MATRIX FORMULATION

To utilize the transfer matrix technique, we consider two specific geometries: slabs and semi-infinite systems. In these two situations, one particular dimension, which we refer to as the vertical direction, features terminations on one or both sides. Then, assuming periodicity along all other dimensions, we will have one or two surfaces for slabs and semi-infinite solids, respectively. We further assume a layered structure along the vertical direction as depicted in Fig. 1, where there are only nearest-neighbor couplings between adjacent layers. It is worth noting that even when this condition is not directly fulfilled by the original tight-binding model, we have the flexibility to redefine the layers, as long as the model primarily consists of short-range hopping terms between physical atomic layers.

Under the above conditions, the tight-binding model can be equivalently described by a set of coupled recursive equations

$$(\varepsilon - \mathcal{M}) |\psi_n(\mathbf{k}_{\parallel})\rangle = \mathcal{T} |\psi_{n+1}(\mathbf{k}_{\parallel})\rangle + \mathcal{T}^{\dagger} |\psi_{n-1}(\mathbf{k}_{\parallel})\rangle, \quad (1)$$

where matrices \mathcal{M} and \mathcal{T} represent intra- and inter-layer hoppings, respectively. Both of these matrices explicitly depend on the transverse momentum \mathbf{k}_{\parallel} provided that we have periodicity in all transverse directions. For non-singular inter-layer hopping matrix \mathcal{T} , we can recast the equation above as

$$\begin{pmatrix} |\psi_{n+1}(\mathbf{k}_{\parallel})\rangle \\ |\psi_n(\mathbf{k}_{\parallel})\rangle \end{pmatrix} = \mathbb{T} \begin{pmatrix} |\psi_n(\mathbf{k}_{\parallel})\rangle \\ |\psi_{n-1}(\mathbf{k}_{\parallel})\rangle \end{pmatrix}, \quad (2)$$

which basically defines the transfer matrix

$$\mathbb{T}(\varepsilon, \mathbf{k}_{\parallel}) = \begin{pmatrix} \mathcal{T}^{-1}(\varepsilon - \mathcal{M}) & -\mathcal{T}^{-1}\mathcal{T}^{\dagger} \\ \mathbb{1} & 0 \end{pmatrix}. \quad (3)$$

For a model with μ different bands, the transfer matrix \mathbb{T} is a $2\mu \times 2\mu$ matrix. The special case of non-invertible \mathcal{T} such that $\mathcal{T}^2 = 0$ (or more generally $\mathcal{T}^l = 0$ for some integer $l > 1$.) has been extensively explored in [18, 19]. Here we will mostly rely on the more generic and common cases where $\det \mathcal{T} \neq 0$. Nonetheless, as we will see in the following, we can still obtain the surface states of the system even when \mathcal{T} is not invertible. To this end, we slightly modify the transfer matrix equation (2) as

$$\mathbb{R} \begin{pmatrix} |\psi_{n+1}(\mathbf{k}_{\parallel})\rangle \\ |\psi_n(\mathbf{k}_{\parallel})\rangle \end{pmatrix} = \mathbb{S} \begin{pmatrix} |\psi_n(\mathbf{k}_{\parallel})\rangle \\ |\psi_{n-1}(\mathbf{k}_{\parallel})\rangle \end{pmatrix}, \quad (4)$$

with

$$\mathbb{S} = \begin{pmatrix} \varepsilon - \mathcal{M} & -\mathcal{T}^{\dagger} \\ \mathbb{1} & 0 \end{pmatrix}, \quad \mathbb{R} = \begin{pmatrix} \mathcal{T} & 0 \\ 0 & \mathbb{1} \end{pmatrix}, \quad (5)$$

where both matrices \mathbb{S} and \mathbb{R} are explicit functions of energy ε and transverse momentum \mathbf{k}_{\parallel} . One can readily check that Eq. (5) is basically equivalent to Eq. (2) yet more generic as it does not require \mathcal{T} to be invertible.

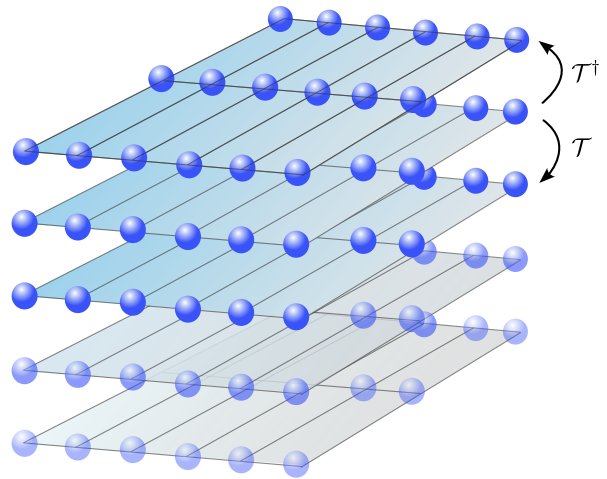


FIG. 1. A schematic illustration of layered atomic structure used to construct the recursive relations of inter-layer couplings, from which the transfer matrix is constructed. \mathcal{T} and \mathcal{T}^{\dagger} denote the hopping matrix between adjacent layers.

Typically, by diagonalizing the transfer matrix \mathbb{T} , we can obtain the electronic structure of the system including boundary modes or surface states which are localized at the boundaries and exponentially vanishes by going deep into the bulk [23]. As one expects, the eigen-solutions of the transfer matrix (3) are the same as the generalized eigenvalue problem corresponding to Eq. (4) as

$$\mathbb{S} |\Phi_{\alpha}\rangle = \lambda_{\alpha} \mathbb{R} |\Phi_{\alpha}\rangle. \quad (6)$$

By plugging in the matrix structure given by Eq. (5), we see that all eigenstates can be decomposed to two sub-columns as

$$|\Phi_{\alpha}\rangle = \begin{pmatrix} \lambda_{\alpha} |\varphi_{\alpha}\rangle \\ |\varphi_{\alpha}\rangle \end{pmatrix}, \quad (7)$$

which gives rise to

$$\lambda_{\alpha} [(\varepsilon - \mathcal{M}) - \mathcal{T} \lambda_{\alpha}] |\varphi_{\alpha}\rangle - \mathcal{T}^{\dagger} |\varphi_{\alpha}\rangle = 0, \quad (8)$$

and a corresponding characteristic equation

$$\det [\lambda^2 \mathcal{T} - \lambda (\varepsilon - \mathcal{M}) + \mathcal{T}^{\dagger}] = 0. \quad (9)$$

In the next section, we will use this to obtain the surface states of some well-known tight-binding models hosting topological phases.

Since we are dealing with a static time-independent setting, the conservation of the current density requires that the transfer matrix has a determinant equal to unity. Furthermore, one can show that the eigenvalues of the transfer matrix consists of pairs of complex numbers λ_{α} and $\lambda_{\alpha'}$ with the property $(\lambda_{\alpha}^* \lambda_{\alpha'} = 1)$ [23], meaning that for any given eigenvalue λ , there must be a complementary eigenvalue $1/\lambda^*$. This becomes very crucial in finding the surface states of the system which decay

from the surface into the bulk of the material. In fact, surface states correspond to eigenvalues whose absolute value is smaller than unity ($|\lambda_\alpha| < 1$) in semi-infinite geometry as considered here. Due to the above condition, there are exactly equal number of eigenvalues of with absolute value larger than unity ($|\lambda_\alpha| > 1$), which can be interpreted as surface states of a complementary system where the surface is located at the opposite end of the semi-infinite geometry. The bulk states correspond to the eigenvalues with unit absolute value ($|\lambda_\alpha| = 1$) which are not localized on surfaces. Now, quite generally, we can always divide the diagonalizing matrix of the \mathbb{T} into two parts as

$$\mathcal{V}_{\mathbb{T}} = (\mathcal{V}_{\leq 1}, \mathcal{V}_{\geq 1}) \quad (10)$$

where $\mathcal{V}_{\leq 1}$ and $\mathcal{V}_{\geq 1}$ are matrices with dimensions $2\mu \times \mu$ whose columns are the eigenvectors of \mathbb{T} corresponding to the eigenvalues with absolute values smaller and larger than unity, respectively (For those eigenvalues which $|\lambda_\alpha| = 1$ the division would be quite arbitrary). One natural choice in the above decomposition is to sort the eigenvalues in ascending order based on their absolute values, such that

$$\mathcal{V}_{\leq 1} = (|\Phi_1\rangle, \dots, |\Phi_\mu\rangle), \quad (11)$$

$$\mathcal{V}_{\geq 1} = (|\Phi_{\mu+1}\rangle, \dots, |\Phi_{2\mu}\rangle). \quad (12)$$

Then, the most generic solution for the surface states of the system reads

$$|\Psi_n\rangle_{\text{sur}} = \begin{pmatrix} |\psi_{n+1}\rangle \\ |\psi_n\rangle \end{pmatrix} = \sum_{\alpha=1}^{\mu} c_\alpha \lambda_\alpha^n |\Phi_\alpha\rangle, \quad (13)$$

with coefficients c_α . At this point, it is worth reminding that both the eigenvalues and eigenvectors are functions of the transverse momentum \mathbf{k}_\parallel and the energy ε . In order to have a complete set of equations from which we can obtain unique solutions for the surface states and their corresponding energies, we would also require boundary conditions. Assuming surface termination of the system at $n = 0$, such that $|\psi_{-1}\rangle = 0$, Eq. (1) at the surface reduces to

$$(\varepsilon - \mathcal{M}) |\psi_0(\mathbf{k}_\parallel)\rangle = \mathcal{T} |\psi_1(\mathbf{k}_\parallel)\rangle, \quad (14)$$

which serves as the boundary condition for the surface states. We can re-write Eq. (14) invoking the surface states expression given by Eq. (13) as

$$\begin{aligned} & (-\mathcal{T}, \varepsilon - \mathcal{M}) |\Psi_0\rangle_{\text{sur}} \\ &= \sum_{\alpha=1}^{\mu} (-\mathcal{T}, \varepsilon - \mathcal{M}) |\Phi_\alpha\rangle c_\alpha \\ &= (-\mathcal{T}, \varepsilon - \mathcal{M}) \mathcal{V}_{\leq 1} \{c_\mu\} = 0, \end{aligned} \quad (15)$$

with $\{c_\mu\}$ being the column vector consisting of coefficients c_α ($1 \leq \alpha \leq \mu$). The above equation can have nontrivial solutions ($\{c_\mu\} \neq 0$) only if

$$\det [(-\mathcal{T}, \varepsilon - \mathcal{M}) \mathcal{V}_{\leq 1}] = 0, \quad (16)$$

from which the surface state energies ε_{sur} can be obtained. The decaying surface states criterion given by Eq. (16) can be further simplified to

$$\det \left[\frac{1}{\lambda_1} |\varphi_1\rangle, \dots, \frac{1}{\lambda_\mu} |\varphi_\mu\rangle \right] = 0, \quad (17)$$

where we have used Eqs. (7) and (8). The surface state energies ε_{sur} can be obtained using the above relation which serves as the decay condition for the surface states.

III. RESULTS

This section presents the exact results for the surface states of two important lattice models used to study topological insulating and metallic phases: (a) the BHZ model and (b) the two-band model for Weyl semimetals, derived using our transfer matrix formulation. We also consider the slab geometry composed of multiple layers for both models and numerically compute the dispersion relations using exact diagonalization of their tight-binding Hamiltonians. The transfer matrix results show complete agreement with the numerical results for sufficiently wide slabs, not only for the surface states but also for the projection of bulk bands across the entire 2D Brillouin zone of the surface.

A. 3D Bernevig-Hughes-Zhang model

We first consider the 3D BHZ model given by the lattice-regularized Hamiltonian [11, 12, 27],

$$\mathcal{H}_{\text{BHZ}}(\mathbf{k}) = M_{\mathbf{k}} \Gamma_0 + 2 \sum_{i=1}^3 \lambda_i \sin k_i \Gamma_i \quad (18)$$

with Gamma matrices $\Gamma_0 = \sigma_0 \otimes \tau_z$, $\Gamma_1 = \sigma_z \otimes \tau_x$, $\Gamma_2 = \sigma_0 \otimes \tau_y$, $\Gamma_3 = \sigma_x \otimes \tau_x$ (all terms are mutually anti-commuting). The diagonal terms are given by energy expression $M_{\mathbf{k}} = m - 2 \sum_i t_i \cos k_i$. Using the generic expression for the bulk states of the multi-band model given in App. A, the bulk state energies of the 3D BHZ model read

$$\varepsilon_{\mathbf{k}}^{\text{bulk}} = \pm \sqrt{M_{\mathbf{k}}^2 + 4 \sum_{i=1}^3 \lambda_i^2 \sin^2 k_i}. \quad (19)$$

This Hamiltonian can show weak and strong topological phases as well as a trivial insulating phase [27]. Assuming all equal hopping terms $t_i = t$, the strong topological phase (STP) which is robust against disorder appears for $2 < |m/t| < 6$ with surface states at the vicinity of Γ point. The weak topological phase (WTP) exist for $|m/t| < 2$ with surface modes at the vicinity of X point. The system undergoes gap closing and topological phase transitions at $|m/t| = 2, 6$ and we have a trivial phase when $|m/t| > 6$.

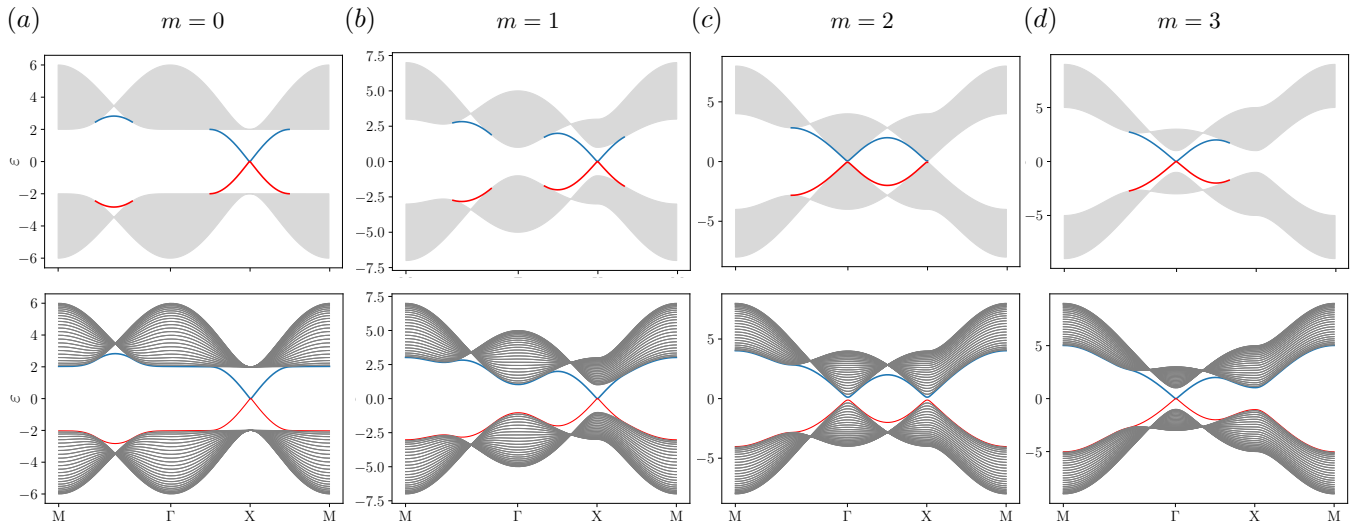


FIG. 2. Band structure of surface states and bulk modes of the 3D BHZ model. The energies are shown along the path between high symmetry points Γ , M, and X in the surface-projected 2D Brillouin zone. The upper panels show the analytical results obtained from the transfer matrix technique, and the lower panels are corresponding results calculated from the direct numerical solution of a tight-binding model in a slab geometry with 50 layers parallel to the surface. The bulk bands are in grey and the surface states are shown in red and blue.

Considering a slab geometry with surfaces parallel to z direction, the transfer matrix can be constructed by re-writing the expressions for the momentum-dependent coefficients of the Hamiltonian by treating the terms involving momentum k_y as the translation operators $T_{\pm y}$. This then leads to the recursive Eq. (1) with

$$\mathcal{M} = m_{\mathbf{k}}\Gamma_0 + 2 \sum_{i=1}^2 \lambda_i \sin k_i, \quad (20)$$

$$\mathcal{T} = -(t_z\Gamma_0 + i\lambda_z\Gamma_3), \quad (21)$$

in which $m_{\mathbf{k}} = M_{\mathbf{k}} + 2t_z \cos k_z = m - 2 \sum_{i=1}^2 t_i \cos k_i$.

Following the recipe of previous section for transfer matrix and as detailed in the App. B, we finally find the following relation

$$-4\nu m_{\mathbf{k}} \pm \theta (m_{\mathbf{k}}^2 - 4(\nu + 1)) + 2\theta^2 m_{\mathbf{k}} \pm \theta^3 = 0, \quad (22)$$

for the energies of surface states and projected bulk states of the 3D BHZ Hamiltonian. Here, the energy dependency comes through the term $\theta = \sqrt{\varepsilon^2 - |\Lambda_{\mathbf{k}}|^2}$ with $\Lambda_{\mathbf{k}} = 2(\lambda_x \sin k_x + i\lambda_y \sin k_y)$. The other two parameters are given by $m_{\mathbf{k}} = m - 2 \sum_{i=1,2} t_i \cos k_i$ and $\nu = (t_z^2 - \lambda_z^2)/t_z$. Note that we have considered the termination in the z -direction such that the surface states are localized at the $z = 0$ surface, for instance. Eq. (22) which is a cubic equation for θ can be solved to obtain the surface state energies. But the full expression of the solutions in generic cases are quite lengthy and therefore, they are only presented in the App. B.

Considering a special case of $\lambda_z = \pm t_z$ which implies $\nu = 0$, the solutions for θ are $\theta = 0$, and $\theta = \pm(m_{\mathbf{k}} \pm 2)$. Substituting these results into the expression of transfer

matrix eigenvalues λ , we find that only the solutions with $\theta = 0$ are proper surface states with decaying nature for which λ is $m_{\mathbf{k}}$ or $1/m_{\mathbf{k}}$ depending on whether $m_{\mathbf{k}} < 1$ or $m_{\mathbf{k}} > 1$, respectively. Therefore, surface state energies for the 3D BHZ model reads,

$$\varepsilon^{\text{sur}}(k_x, k_y) = \pm \Lambda_{\mathbf{k}} = \pm 2 \sqrt{\lambda_x^2 \sin^2 k_x + \lambda_y^2 \sin^2 k_y}. \quad (23)$$

We can also check that the bulk states maximum and minimum energies, when projected onto the 2D Brillouin zone of the surface, are given by

$$\begin{aligned} \varepsilon^{\text{bulk}}(k_x, k_y) &= \pm \sqrt{\Lambda_{\mathbf{k}}^2 + (m_{\mathbf{k}} \pm 2)^2} \\ &= \pm 2 \sqrt{\lambda_x^2 \sin^2 k_x + \lambda_y^2 \sin^2 k_y + \left(\frac{m_{\mathbf{k}}}{2} + \pm 1\right)^2}, \end{aligned} \quad (24)$$

where we have all four possible combinations of the two signs which correspond to four energy dispersion relations. It is noteworthy that the maximum and minimum energies of bulk states can be determined through two distinct methods. Firstly, they can be obtained by inspecting the energy expression of bulk states, as given in Eq. (24). Secondly, and more intriguingly, the energy band edges can also be derived from alternative solutions for θ , wherein the transfer matrix eigenvalue reaches unit amplitude ($|\lambda| = 1$). This indicates that these solutions exhibit non-decaying characteristics, effectively representing bulk states projected onto the 2D Brillouin zone of the surface.

We now compare analytical expressions for the surface states and bulk band edges projected onto the surface Brillouin zone with those obtained from direct numerical

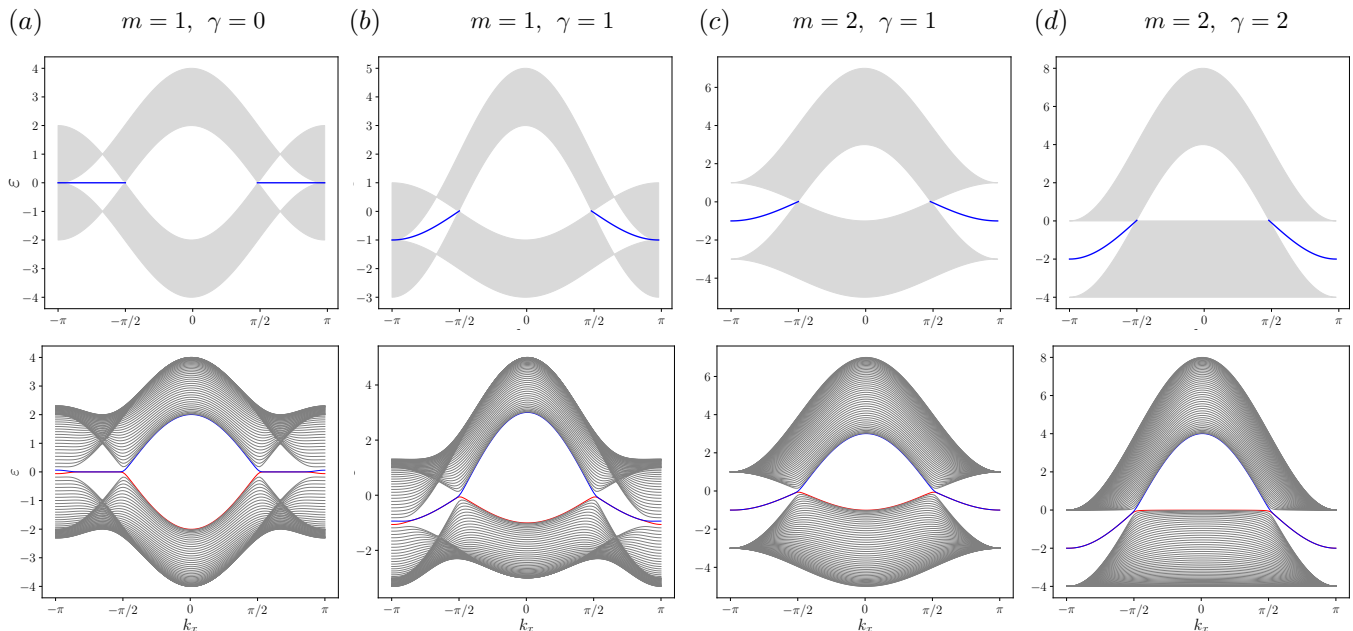


FIG. 3. Band structure of surface states and bulk modes of the 3D simple Weyl model consisting of only two bands. Similar to Fig. 2, the upper panels show the analytical results obtained from the transfer matrix technique, and the lower panels show the corresponding results calculated from the direct numerical solution. The bulk bands are in grey and Fermi arc states (surface modes) are shown in blue.

diagonalization as presented in Fig. 2. For the numerical analysis, we considered the tight-binding Hamiltonians for a slab geometry consisting of 50 layers. The hopping parameters were set to $t_i = \lambda_i = 1$, and the mass parameter m was varied to explore different phases of the model (WTP, STP, and trivial insulator). As illustrated in the figure, the analytical expressions perfectly match the numerical results. Panels (a) and (b) display the WTP with surface states localized at the X point. Panel (c) represents the gap closing point, marking the transition from the WTP to the STP, which is further shown in panel (d).

B. Weyl semimetal model

The minimal lattice model for a WSM consisting of two bands and only two Weyl nodes is given by [28]

$$\hat{\mathcal{H}}_{\text{WSM-I}}(\mathbf{k}) = \sum_{i=0}^3 d_i(\mathbf{k}) \hat{\sigma}_i, \quad (25)$$

where

$$\begin{aligned} d_0 &= \gamma[\cos(k_x) - \cos(k_0)], \\ d_1 &= m[\cos(k_y) + \cos(k_z) - 2] \\ &\quad + 2t_x[\cos(k_0) - \cos(k_x)], \\ d_2 &= -2t \sin(k_y), \\ d_3 &= -2t \sin(k_z). \end{aligned} \quad (26)$$

The bulk band energies dispersion for this model is

$$\varepsilon_{\mathbf{k}}^{\text{bulk}} = d_0 \pm \sqrt{\sum_{i=1}^3 d_i^2} \quad (27)$$

This simple model also has the advantage of exhibiting a transition between type I and II WSMs.

Assuming a finite slab geometry with surfaces parallel to y direction, and introducing translation operator similar to the previous example, the intra- and inter-layer terms of the recursive relation for the wavefunction components are given by $\mathcal{T} = \frac{m}{2} \hat{\sigma}_1 + it \hat{\sigma}_2$ and $\mathcal{M} = d_0(\mathbf{k}) \hat{\sigma}_0 + h_1(\mathbf{k}) \hat{\sigma}_1 + d_3(\mathbf{k}) \hat{\sigma}_3$ where

$$\begin{aligned} h_1 &= d_1 - m \cos(k_y) \\ &= -m[2 - \cos(k_z)] - 2t_x[\cos(k_x) - \cos(k_0)]. \end{aligned} \quad (28)$$

Applying the formulation of Sec. II as detailed in App. C, the dispersion of Fermi arc states and projection of bulk states to the surface Brillouin zone are given by

$$\varepsilon^{\text{sur}}(k_x, k_z) = d_0 \pm |d_3|, \quad (29)$$

$$\varepsilon^{\text{bulk}}(k_x, k_z) = d_0 \pm \sqrt{d_3^2 + (h_1 \pm m)^2}, \quad (30)$$

respectively.

The results derived from the analytical equations above, along with those obtained from direct numerical diagonalization of the tight-binding Hamiltonians for a slab geometry consisting of 50 layers, are presented in Fig. 3. The figure illustrates consistency between the

exact expressions and numerical results for the surface modes and the bulk band edges (by projection to the 2D Brillouin zone of the surface).

IV. DISCUSSION

We have developed a modified version of the transfer matrix technique originally proposed by Lee and Joannopoulos [23], which is applicable to both invertible and non-invertible inter-layer coupling matrices \mathcal{T} in tight-binding Hamiltonians. This modification distinguishes our approach from other recent techniques used to explore topological boundary states [18, 19], which specifically focus on the case of non-invertible \mathcal{T} . Our method enables the exact determination of the dispersion relations of topological surface states in several well-known models for 3D topological insulators, including the 3D BHZ model, as well as models exhibiting Weyl semimetallic behavior. The success of our method in providing exact expressions for surface states using the transfer matrix technique still depends on the exact solvability of the eigenvalue equations and the boundary conditions. In particular, increasing the number of bands leads to larger matrices and higher-degree secular equations. Since polynomial equations of degree five or higher do not generally have exact solutions, there is no guarantee that exact surface dispersion relations can always be found.

Alternatively, a numerical framework based on the transfer matrix can be used instead of numerically diagonalizing real-space Hamiltonians for finite geometries in one direction. The computational complexity of the transfer matrix method scales with the size of the matrix \mathbb{T} (i.e., twice the number of bands), while direct numerical methods scale with the product of the number of bands and the number of layers in the slab geometry. This not only makes the transfer matrix method significantly more efficient but also possibly the only practical approach for semi-infinite or very wide geometries. Because diagonalization of the real-space Hamiltonian is limited to finite-sized slabs and requires size-scaling analysis to extrapolate results for surface states in semi-infinite or very wide geometries. In contrast, the transfer matrix method allows for exact analytical or numerical analysis of surface physics, which surpasses brute-force approaches, particularly when dealing with semi-infinite geometries or isolated surface states. The development of a numerical method based on the transfer matrix is left for a future work.

Now, our results can be employed to investigate surface physics and interfaces involving topological phases, providing valuable insights into the surface physics of various topological states beyond the low-energy limit. Specifically, the analytical results for the surface states dispersion throughout the surface Brillouin zone can be applied to explore engineered topological phases at the interfaces and heterostructures. These interfaces, where different

topological phases or a topological insulator and a conventional material interact, can give rise to novel quantum states [29–37], and hold promise for electronics and spintronics application [38–41]. Such engineered phases are particularly significant in the context of topological superconductivity, where the proximity effect between a superconductor and a topological insulator can induce a superconducting phase that inherits the topological properties [42–51].

As a concrete example, one can construct an effective model of the interface based on the exact surface dispersions derived here and introduce the effective superconducting pairing between them. This will elevate the model beyond the typical studies using the low-energy dispersion of surface modes and typically approximated by an effective Dirac Hamiltonian. Furthermore, it bridges the gap between effective low-energy models and fully numerical models based on tight-binding or ab initio methods, enabling a more comprehensive exploration of interface-induced topological superconductivity. Similar approaches can be applied to other engineered topological phases at boundaries a topological material and a non-topological system. A notable example is interfacial magnetic topological insulators formed by the proximity of time-reversal-invariant 3D topological insulators and materials with magnetic ordering.

V. SUMMARY

In conclusion, we have developed an exact formalism for deriving topological surface states and Fermi arc states in 3D tight-binding lattice models that exhibit topological insulating and semimetallic behaviors. By introducing a generalized eigenvalue problem involving two matrices, \mathbb{S} and \mathbb{R} such that $\mathbb{R}\mathbb{T} = \mathbb{S}$, where \mathbb{R} with \mathbb{T} represents the transfer matrix, we address the non-invertibility issue caused by the inter-layer hopping term, often encountered in the standard transfer matrix approach. This formulation allows us to decompose both surface and bulk states in terms of the eigenstates of this generalized eigenvalue problem, serving as a substitute for the traditional transfer matrix method. By applying boundary conditions for surface termination, we derive analytical expressions for surface state energies and the edges of bulk bands in the projected 2D Brillouin zone. Our method has been successfully applied to well-known models such as the 3D Bernevig-Hughes-Zhang model and a widely studied two-band model for Weyl semimetals. These analytical results provide a more efficient alternative to fully numerical methods, particularly in cases requiring surface state properties beyond the low-energy regimes.

Appendix A: Bulk states of the generic multi-band model

We consider a set of mutually anti-commuting gamma matrices Γ_i which square to identity which is divided into two sets $\{\Gamma_i^{(1)}\}$, $\{\Gamma_j^{(2)}\}$, respectively. The anti-commutation relations are given by

$$\{\Gamma_i^{(q)}, \Gamma_j^{(q')}\} = 2\delta_{ij}\delta_{qq'} \mathbb{1}, \quad (\text{A1})$$

So far the division of the gamma matrices into two sets seems arbitrary. Now we assume there are two extra matrices $\Xi^{(1)}$ and $\Xi^{(2)}$ which *commute* with each other ($[\Xi^{(1)}, \Xi^{(2)}] = 0$) and square to identity. Additionally, we have commutation and anti-commutation relations between $\Xi^{(q)}$ and $\Gamma_i^{(q')}$ as follows:

$$[\Xi^{(q)}, \Gamma_i^{(q)}] = 0, \quad (\text{A2})$$

$$\{\Xi^{(q)}, \Gamma_i^{(q')}\} = 0, \quad (q \neq q') \quad (\text{A3})$$

Then, we can write the generic k -space Hamiltonian expressed in terms of all these gamma matrices and an additional identity term as

$$\mathcal{H} = \delta \mathbb{1} + \sum_{q=1,2} \left(\mathbf{h}_q \cdot \Gamma^{(q)} + \xi_q \Xi^{(q)} \right), \quad (\text{A4})$$

where coefficients $\mathbf{h}_q = h_{q,i} \hat{\mathbf{e}}_i$ and $\xi^{(q)}$ depend on the momentum \mathbf{k} . Now, as we will see below, the energy spectrum of this Hamiltonian can be exactly obtained in terms of the coefficients $h_i^{(q)}$ and $\xi^{(q)}$. To this end, we first take the square of the Hamiltonian after subtracting the identity term $\delta \mathbb{1}$ as

$$\begin{aligned} (\mathcal{H} - \delta \mathbb{1})^2 &= \left(\sum_{q=1,2} \mathbf{h}_q \cdot \Gamma^{(q)} \right)^2 + \left(\sum_{q=1,2} \xi_q \Xi^{(q)} \right)^2 \\ &+ \sum_{q,q'=1,2} \left\{ \mathbf{h}_q \cdot \Gamma^{(q)}, \xi_{q'} \Xi^{(q')} \right\} \end{aligned} \quad (\text{A5})$$

$$\begin{aligned} &= \sum_{q=1,2} (|\mathbf{h}_q|^2 + |\xi_q|^2) \mathbb{1} + 2\xi_1 \xi_2 \Xi^{(1)} \Xi^{(2)} \\ &+ 2 \sum_{q=1,2} \xi_q \Xi^{(q)} \mathbf{h}_q \cdot \Gamma^{(q)}, \end{aligned} \quad (\text{A6})$$

where to obtain the last line we have used the anti-commutation and commutation relations between different matrices. Let's bring the first term of the last line, which is proportional to identity, to the left-hand side and square it again. This results in

$$\begin{aligned} &\frac{1}{4} \left[(\mathcal{H} - \delta \mathbb{1})^2 - \sum_{q=1,2} (|\mathbf{h}_q|^2 + |\xi_q|^2) \mathbb{1} \right]^2 \\ &= \left(\sum_{q=1,2} \xi_q \Xi^{(q)} \mathbf{h}_q \cdot \Gamma^{(q)} \right)^2 + \xi_1^2 \xi_2^2 \mathbb{1} \\ &+ \left\{ \sum_{q=1,2} \xi_q \Xi^{(q)} \mathbf{h}_q \cdot \Gamma^{(q)}, \xi_1 \xi_2 \Xi^{(1)} \Xi^{(2)} \right\}, \end{aligned} \quad (\text{A7})$$

where we have used the fact that $(\Xi^{(1)} \Xi^{(2)})^2 = \mathbb{1}$. As we can easily verify, the new sets of matrices given by $\Xi^{(q)} \Gamma_i^{(q)}$ are also mutually anti-commuting and square to identity as

$$\left\{ \Xi^{(q)} \Gamma_i^{(q)}, \Xi^{(q')} \Gamma_j^{(q')} \right\} = 2\delta_{ij}\delta_{qq'} \mathbb{1}. \quad (\text{A8})$$

Therefore, the first term on the right-hand side of Eq. (A7) simplifies to

$$\left(\sum_{q=1,2} \xi_q \Xi^{(q)} \mathbf{h}_q \cdot \Gamma^{(q)} \right)^2 = \sum_{q=1,2} \xi_q^2 |\mathbf{h}_q|^2 \mathbb{1}. \quad (\text{A9})$$

Furthermore, as one can verify by direct inspection, the last term in the right-hand side of Eq. (A7) vanishes identically. Therefore, we have

$$\begin{aligned} &\frac{1}{4} \left[(\mathcal{H} - \delta \mathbb{1})^2 - \sum_{q=1,2} (|\mathbf{h}_q|^2 + |\xi_q|^2) \mathbb{1} \right]^2 \\ &= \left(\sum_{q=1,2} \xi_q^2 |\mathbf{h}_q|^2 + \xi_1^2 \xi_2^2 \right) \mathbb{1}. \end{aligned} \quad (\text{A10})$$

Since all the matrices apart from the Hamiltonian are now proportional to identity, we can deduce the characteristic equation for the eigenvalues of the Hamiltonian as [52],

$$\begin{aligned} (\varepsilon - \delta)^2 - \sum_q (\xi_q^2 + |\mathbf{h}_q|^2) &= \\ \pm 2 \sqrt{\sum_q \xi_q^2 |\mathbf{h}_q|^2 + \xi_1^2 \xi_2^2}, \end{aligned} \quad (\text{A11})$$

and therefore the energies are given by

$$\begin{aligned} \varepsilon_{\zeta\zeta'} &= \delta + \zeta \\ &\times \sqrt{\sum_q (\xi_q^2 + |\mathbf{h}_q|^2) + 2\zeta' \sqrt{\sum_q \xi_q^2 |\mathbf{h}_q|^2 + \xi_1^2 \xi_2^2}}. \end{aligned} \quad (\text{A12})$$

Appendix B: Transfer matrix for the 3D BHZ model

We first work out the characteristic equation for the transfer matrix eigenvalues by inserting the matrices \mathcal{M} and \mathcal{T} of 3D BHZ model into Eq. (9) and evaluating it which results in:

$$\left[-\frac{\nu}{2} (\lambda^4 + 1) + m_{\mathbf{k}} (\lambda^3 + \lambda) + \lambda^2 (\nu - \zeta) \right]^2 = 0, \quad (\text{B1})$$

in which

$$\nu = \frac{t_z^2 - \lambda_z^2}{t_z}, \quad (\text{B2})$$

$$\zeta = \frac{m_{\mathbf{k}}^2 + 4t_z^2 - \varepsilon^2 + |\Lambda_{\mathbf{k}}|^2}{2t_z}, \quad \Lambda_{\mathbf{k}} = 2 \sum_{i=1}^2 \lambda_i \sin k_i. \quad (\text{B3})$$

The solutions of the characteristic equation above are all two-fold degenerate and can be written as

$$\begin{aligned}\lambda_{1,2} &= \frac{1}{2} \left(\chi_+ \pm \sqrt{\chi_+^2 - 4} \right) \\ \lambda_{3,4} &= \frac{1}{2} \left(\chi_- \pm \sqrt{\chi_-^2 - 4} \right),\end{aligned}\quad (\text{B4})$$

where χ_{\pm} are the two roots of

$$-\frac{\nu}{2} \chi^2 + m_{\mathbf{k}} \chi + (2\nu - \zeta) = 0, \quad (\text{B5})$$

For any λ we have two different eigenstate whose lower part using the decomposition in (7) are

$$|\varphi\rangle_{1,\lambda} \propto \begin{pmatrix} (\lambda^2 - 1)\lambda_z \\ 0 \\ -i\lambda\Lambda_{\mathbf{k}} \\ it_z(1 + \lambda^2) + i\lambda(\varepsilon - m_{\mathbf{k}}) \end{pmatrix}, \quad (\text{B6})$$

and

$$|\varphi\rangle_{2,\lambda} \propto \begin{pmatrix} 0 \\ (\lambda^2 - 1)\lambda_z \\ -it_z(1 + \lambda^2) + i\lambda(\varepsilon + m_{\mathbf{k}}) \\ -i\lambda\Lambda_{\mathbf{k}} \end{pmatrix}. \quad (\text{B7})$$

Now, the decaying surface state criteria (boundary condition) described by Eq. (17), by plugging the eigenstate $|\varphi\rangle_{i,\lambda}$ and after some algebraic manipulations reduces to

$$\frac{\lambda_1 + \lambda_2}{\lambda_1 \lambda_2 + 1} = \frac{m_{\mathbf{k}} \pm \sqrt{\varepsilon^2 - |\Lambda_{\mathbf{k}}|^2}}{2t}, \quad (\text{B8})$$

Invoking the expressions for the transfer matrix eigenvalues and after some algebra, we find

$$-4\nu m_{\mathbf{k}} \pm \theta (m_{\mathbf{k}}^2 - 4(\nu + 1)) + 2\theta^2 m_{\mathbf{k}} \pm \theta^3 = 0, \quad (\text{B9})$$

where $\theta = \sqrt{\varepsilon^2 - |\Lambda_{\mathbf{k}}|^2}$.

As the two equations are simply related to each other by $\theta \rightarrow -\theta$, we can focus only on the equation with positive signs, and the solutions for the other equations are simply obtained by changing the signs. For the particular case of $\nu = 0$, the equation can be easily factorized as

$$\pm\theta[(\theta \pm m_{\mathbf{k}})^2 - 4] = 0, \quad (\text{B10})$$

with five different solutions $\theta = 0$, and $\theta = \pm 2 \pm m_{\mathbf{k}}$.

For the generic case ($\nu \neq 0$), we first simplify the equation by absorbing the quadratic term via defining a new variable

$$\phi = \theta + \frac{2}{3}m_{\mathbf{k}}, \quad (\text{B11})$$

in terms of which the equation becomes

$$\phi^3 - \phi \left(4(\nu + 1) + \frac{m_{\mathbf{k}}^2}{3} \right) - \frac{2}{27}m_{\mathbf{k}} (18(\nu - 2) + m_{\mathbf{k}}^2) = 0. \quad (\text{B12})$$

This new equation has the form of the *depressed cubic equation*

$$\phi^3 + 3p\phi - 2q = 0, \quad (\text{B13})$$

whose solutions are given by

$$\phi = \begin{cases} z_- - z_+ \\ e^{2\pi i/3} z_- - e^{-2\pi i/3} z_+ \\ e^{-2\pi i/3} z_- - e^{2\pi i/3} z_+ \end{cases}, \quad (\text{B14})$$

where

$$z_{\pm} = (\sqrt{q^2 + p^3} \pm q)^{1/3}. \quad (\text{B15})$$

The two parameter q and p can be obtained by comparing Eqs. (B12) and (B13) as

$$p = -\frac{1}{3} \left(4(\nu + 1) + \frac{m_{\mathbf{k}}^2}{3} \right), \quad (\text{B16})$$

$$q = \frac{1}{27}m_{\mathbf{k}} (18(\nu - 2) + m_{\mathbf{k}}^2). \quad (\text{B17})$$

So the combination of expressions given by Eqs. (B14)-(B17) determines the solutions for the variable ϕ , and thereby the energies.

Appendix C: Transfer matrix for the simple Weyl model

The generalized eigenvalue form of the transfer matrix for simple Weyl model (25) can be written as the following

$$\mathbb{S} - \lambda \mathbb{R} = \begin{pmatrix} \xi + d_3 & \lambda m_+ + h_1 & 0 & m_- \\ \lambda m_- + h_1 & \xi - d_3 & m_+ & 0 \\ 1 & 0 & -\lambda & 0 \\ 0 & 1 & 0 & -\lambda \end{pmatrix}, \quad (\text{C1})$$

in which the following variables are defined for the sake of compactness:

$$\begin{aligned}\xi &= \varepsilon - d_0(k_x) = \varepsilon - \gamma[\cos(k_x) - \cos(k_0)], \\ h_1 &= -m[2 - \cos(k_z)] - 2t_x[\cos(k_x) - \cos(k_0)], \\ d_3 &= 2t \sin k_z, \\ m_{\pm} &= \frac{m}{2} \pm t\end{aligned}\quad (\text{C2})$$

The transfer matrix eigenvalues are then found as

$$\begin{aligned}\lambda_{1,2} &= \frac{1}{2} \left(\chi_+ \pm \sqrt{\chi_+^2 - 4} \right) \\ \lambda_{3,4} &= \frac{1}{2} \left(\chi_- \pm \sqrt{\chi_-^2 - 4} \right),\end{aligned}\quad (\text{C3})$$

where

$$\chi_{\pm} = \frac{\pm \sqrt{4t^2 h_1^2 - (m^2 - 4t^2)(-\xi^2 + 4t^2 + d_3^2)} - m h_1}{m^2/2 - 2t^2}. \quad (\text{C4})$$

The corresponding wavefunctions can be decomposed according to (7) in which the lower parts denoted by $|\varphi\rangle$ are also found as

$$|\varphi\rangle_i \propto \begin{pmatrix} \lambda_i^2 m_+ + m_- + \lambda_i h_1 \\ -\lambda_i (d_3 + \xi) \end{pmatrix}. \quad (\text{C5})$$

Using the above wavefunctions and applying the boundary condition (17), we find the criterion

$$\frac{(\lambda_i - \lambda_j)(d_3 + \xi)(\lambda_i \lambda_j m_+ - m_-)}{\lambda_i \lambda_j} = 0 \quad (\text{C6})$$

from which the energies can be obtained.

We first examine solutions of the form $\lambda_i \lambda_j = m_-/m_+$ for non-equal pairs of λ 's. Specifically, considering the condition $\lambda_2 \lambda_4 = m_-/m_+$ and substituting the expressions for the λ 's given by (C3), we find the solution

$$\xi^2 = d_3^2, \quad (\text{C7})$$

which leads to the corresponding energies

$$\varepsilon = \gamma[\cos(k_x) - \cos(k_0)] \pm 2t \sin(k_z). \quad (\text{C8})$$

By substituting these energies into the expressions for the transfer matrix eigenvalues $\lambda_{2,4}$, we verify that they indeed yield decaying solutions over a certain range of momenta, thus corresponding to Fermi arc surface states. Additionally, we observe that inspecting other pairs of λ 's either yields the same result or fails to produce real (physical) solutions for the energies.

The remaining possibility, as indicated by (C6), involves equal pairs of λ 's whose absolute values are both less than or equal to 1. However, since $\chi_1 \neq \chi_2$ for almost any generic set of parameters and momenta, this scenario reduces to either χ_{\pm} being equal to ± 2 , which corresponds to either $\lambda_{1,2} = \pm 1$ or $\lambda_{3,4} = \pm 1$, respectively. Therefore, these solutions correspond to bulk states. By applying the conditions in the expression for χ_{\pm} given in Eq. (C4), we obtain the solutions

$$\xi^2 = d_3^2 + (h_1 \pm m)^2, \quad (\text{C9})$$

which leads to the four energy dispersions

$$\varepsilon = d_0 \pm \sqrt{d_3^2 + (h_1 \pm m)^2}, \quad (\text{C10})$$

corresponding to the bulk band edges.

-
- [1] Alexei Kitaev, "Periodic table for topological insulators and superconductors," *AIP Conference Proceedings* **1134**, 22–30 (2009).
- [2] M. Z. Hasan and C. L. Kane, "Colloquium: Topological insulators," *Rev. Mod. Phys.* **82**, 3045 (2010).
- [3] Xiao-Liang Qi and Shou-Cheng Zhang, "Topological insulators and superconductors," *Rev. Mod. Phys.* **83**, 1057 (2011).
- [4] Shun-Qing Shen, *Topological insulators*, Vol. 174 (Springer, 2012).
- [5] B Andrei Bernevig and Taylor L. Hughes, *Topological insulators and topological superconductors* (Princeton university press, 2013).
- [6] János K Asbóth, László Oroszlány, and András Pályi, "A short course on topological insulators," *Lecture notes in physics* **919**, 166 (2016).
- [7] Ching-Kai Chiu, Jeffrey C. Y. Teo, Andreas P. Schnyder, and Shinsei Ryu, "Classification of topological quantum matter with symmetries," *Rev. Mod. Phys.* **88**, 035005 (2016).
- [8] Yasuhiro Hatsugai, "Chern number and edge states in the integer quantum hall effect," *Phys. Rev. Lett.* **71**, 3697–3700 (1993).
- [9] Shinsei Ryu and Yasuhiro Hatsugai, "Topological Origin of Zero-Energy Edge States in Particle-Hole Symmetric Systems," *Phys. Rev. Lett.* **89**, 077002 (2002).
- [10] Gian Michele Graf and Marcello Porta, "Bulk-edge correspondence for two-dimensional topological insulators," *Comm. Math. Phys.* **324**, 851 (2013).
- [11] Haijun Zhang, Chao-Xing Liu, Xiao-Liang Qi, Xi Dai, Zhong Fang, and Shou-Cheng Zhang, "Topological insulators in Bi₂Se₃, Bi₂Te₃ and Sb₂Te₃ with a single Dirac cone on the surface," *Nat. Phys.* **5**, 438 (2009).
- [12] Chao-Xing Liu, Xiao-Liang Qi, HaiJun Zhang, Xi Dai, Zhong Fang, and Shou-Cheng Zhang, "Model hamiltonian for topological insulators," *Phys. Rev. B* **82**, 045122 (2010).
- [13] Wen-Yu Shan, Hai-Zhou Lu, and Shun-Qing Shen, "Effective continuous model for surface states and thin films of three-dimensional topological insulators," *New Journal of Physics* **12**, 043048 (2010).
- [14] P. G. Silvestrov, P. W. Brouwer, and E. G. Mishchenko, "Spin and charge structure of the surface states in topological insulators," *Phys. Rev. B* **86**, 075302 (2012).
- [15] Fan Zhang, C. L. Kane, and E. J. Mele, "Surface states of topological insulators," *Phys. Rev. B* **86**, 081303 (2012).
- [16] Jeffrey C. Y. Teo, Liang Fu, and C. L. Kane, "Surface states and topological invariants in three-dimensional topological insulators: Application to Bi_{1-x}Sb_x," *Phys. Rev. B* **78**, 045426 (2008).
- [17] M. Neupane, S.-Y. Xu, L. A. Wray, A. Petersen, R. Shankar, N. Alidoust, Chang Liu, A. Fedorov, H. Ji, J. M. Allred, Y. S. Hor, T.-R. Chang, H.-T. Jeng, H. Lin, A. Bansil, R. J. Cava, and M. Z. Hasan, "Topological surface states and dirac point tuning in ternary topological insulators," *Phys. Rev. B* **85**, 235406 (2012).
- [18] Vatsal Dwivedi and Victor Chua, "Of bulk and boundaries: Generalized transfer matrices for tight-binding models," *Phys. Rev. B* **93**, 134304 (2016).
- [19] Flore K. Kunst and Vatsal Dwivedi, "Non-hermitian systems and topology: A transfer-matrix perspective," *Phys. Rev. B* **99**, 245116 (2019).
- [20] Clément Tauber and Pierre Delplace, "Topological edge states in two-gap unitary systems: a transfer matrix approach," *New J. Phys.* **17**, 115008 (2015).
- [21] Vatsal Dwivedi, "Fermi arc reconstruction at junctions

- between weyl semimetals,” *Phys. Rev. B* **97**, 064201 (2018).
- [22] Matthew G Reuter, “A unified perspective of complex band structure: interpretations, formulations, and applications,” *J. Condens. Matter Phys.* **29**, 053001 (2016).
- [23] D. H. Lee and J. D. Joannopoulos, “Simple scheme for surface-band calculations. i,” *Phys. Rev. B* **23**, 4988 (1981).
- [24] Yia-Chung Chang and J. N. Schulman, “Complex band structures of crystalline solids: An eigenvalue method,” *Phys. Rev. B* **25**, 3975 (1982).
- [25] Yasuhiro Hatsugai, “Edge states in the integer quantum hall effect and the riemann surface of the bloch function,” *Phys. Rev. B* **48**, 11851–11862 (1993).
- [26] Xiao-Liang Qi, Yong-Shi Wu, and Shou-Cheng Zhang, “Topological quantization of the spin hall effect in two-dimensional paramagnetic semiconductors,” *Phys. Rev. B* **74**, 085308 (2006).
- [27] L. Crippa, G. Sangiovanni, and J. C. Budich, “Spontaneous formation of exceptional points at the onset of magnetism,” *Phys. Rev. Lett.* **130**, 186403 (2023).
- [28] Timothy M. McCormick, Itamar Kimchi, and Nandini Trivedi, “Minimal models for topological weyl semimetals,” *Phys. Rev. B* **95**, 075133 (2017).
- [29] B Andrei Bernevig, Taylor L Hughes, and Shou-Cheng Zhang, “Quantum spin Hall effect and topological phase transition in HgTe quantum wells,” *Science* **314**, 1757 (2006).
- [30] Markus König, Steffen Wiedmann, Christoph Brune, Andreas Roth, Hartmut Buhmann, Laurens W Molenkamp, Xiao-Liang Qi, and Shou-Cheng Zhang, “Quantum spin Hall insulator state in HgTe quantum wells,” *Science* **318**, 766 (2007).
- [31] Toru Hirahara, Gustav Bihlmayer, Yusuke Sakamoto, Manabu Yamada, Hidetoshi Miyazaki, Shin-ichi Kimura, Stefan Blügel, and Shuji Hasegawa, “Interfacing 2D and 3D Topological Insulators: Bi(111) Bilayer on Bi₂Te₃,” *Phys. Rev. Lett.* **107**, 166801 (2011).
- [32] A. A. Burkov and Leon Balents, “Weyl semimetal in a topological insulator multilayer,” *Phys. Rev. Lett.* **107**, 127205 (2011).
- [33] Weidong Luo and Xiao-Liang Qi, “Massive dirac surface states in topological insulator/magnetic insulator heterostructures,” *Phys. Rev. B* **87**, 085431 (2013).
- [34] Ferhat Katmis, Valeria Lauter, Flavio S Nogueira, Badih A Assaf, Michelle E Jamer, Peng Wei, Biswarup Satpati, John W Freeland, Ilya Eremin, Don Heiman, *et al.*, “A high-temperature ferromagnetic topological insulating phase by proximity coupling,” *Nature* **533**, 513 (2016).
- [35] Bent Weber, Michael S Fuhrer, Xian-Lei Sheng, Shengyuan A Yang, Ronny Thomale, Saquib Shamim, Laurens W Molenkamp, David Cobden, Dmytro Pesin, Harold J W Zandvliet, Pantelis Bampoulis, Ralph Claessen, Fabian R Menges, Johannes Gooth, Claudia Felser, Chandra Shekhar, Anton Tadich, Mengting Zhao, Mark T Edmonds, Junxiang Jia, Maciej Bieniek, Jukka I Väyrynen, Dimitrie Culcer, Bhaskaran Muralidharan, and Muhammad Nadeem, “2024 roadmap on 2d topological insulators,” *J. Phys.: Mater.* **7**, 022501 (2024).
- [36] Tomáš Rauch, Markus Flieger, Jürgen Henk, and Ingrid Mertig, “Nontrivial interface states confined between two topological insulators,” *Phys. Rev. B* **88**, 245120 (2013).
- [37] Panagiotis Kotetes, “Classification of engineered topological superconductors,” *New J. Phys.* **15**, 105027 (2013).
- [38] Cui-Zu Chang, Jinsong Zhang, Xiao Feng, Jie Shen, Zuo Cheng Zhang, Minghua Guo, Kang Li, Yumbo Ou, Pang Wei, Li-Li Wang, *et al.*, “Experimental observation of the quantum anomalous hall effect in a magnetic topological insulator,” *Science* **340**, 167 (2013).
- [39] B Andrei Bernevig, Claudia Felser, and Haim Beidenkopf, “Progress and prospects in magnetic topological materials,” *Nature* **603**, 41 (2022).
- [40] Alex R Mellnik, JS Lee, Anthony Richardella, Jennifer L Grab, Peter J Mintun, Mark H Fischer, Abolhassan Vaezi, Aurelien Manchon, E-A Kim, Nitin Samarth, *et al.*, “Spin-transfer torque generated by a topological insulator,” *Nature* **511**, 449 (2014).
- [41] Ali G. Moghaddam, Alireza Qaiumzadeh, Anna Dyrdał, and Jamal Berakdar, “Highly tunable spin-orbit torque and anisotropic magnetoresistance in a topological insulator thin film attached to ferromagnetic layer,” *Phys. Rev. Lett.* **125**, 196801 (2020).
- [42] Liang Fu and C. L. Kane, “Superconducting proximity effect and majorana fermions at the surface of a topological insulator,” *Phys. Rev. Lett.* **100**, 096407 (2008).
- [43] Yuval Oreg, Gil Refael, and Felix von Oppen, “Helical liquids and majorana bound states in quantum wires,” *Phys. Rev. Lett.* **105**, 177002 (2010).
- [44] Jay D. Sau, Roman M. Lutchyn, Sumanta Tewari, and S. Das Sarma, “Generic new platform for topological quantum computation using semiconductor heterostructures,” *Phys. Rev. Lett.* **104**, 040502 (2010).
- [45] Jason Alicea, “Majorana fermions in a tunable semiconductor device,” *Phys. Rev. B* **81**, 125318 (2010).
- [46] Tudor D. Stanescu, Roman M. Lutchyn, and S. Das Sarma, “Majorana fermions in semiconductor nanowires,” *Phys. Rev. B* **84**, 144522 (2011).
- [47] Vincent Mourik, Kun Zuo, Sergey M Frolov, SR Plissard, Erik PAM Bakkers, and Leo P Kouwenhoven, “Signatures of majorana fermions in hybrid superconductor-semiconductor nanowire devices,” *Science* **336**, 1003 (2012).
- [48] Stevan Nadj-Perge, Ilya K Drozdov, Jian Li, Hua Chen, Sangjun Jeon, Jungpil Seo, Allan H MacDonald, B Andrei Bernevig, and Ali Yazdani, “Observation of majorana fermions in ferromagnetic atomic chains on a superconductor,” *Science* **346**, 602 (2014).
- [49] Masatoshi Sato and Yoichi Ando, “Topological superconductors: a review,” *Rep. Prog. Phys.* **80**, 076501 (2017).
- [50] SM Frolov, MJ Manfra, and JD Sau, “Topological superconductivity in hybrid devices,” *Nat. Phys.* **16**, 718 (2020).
- [51] Karsten Flensberg, Felix von Oppen, and Ady Stern, “Engineered platforms for topological superconductivity and majorana zero modes,” *Nat. Rev. Mater.* **6**, 944 (2021).
- [52] Technically speaking we are applying Cayley–Hamilton theorem, which states any matrix satisfies its own characteristic equation. Therefore, this equation is identical to the characteristic equation $\det(\lambda I - \mathcal{H}) = 0$. whereby, after expanding the determinant, we have replaced the scalar λ with the Hamiltonian matrix.